

See discussions, stats, and author profiles for this publication at: <https://www.researchgate.net/publication/277138099>

The Direct Torque Control of BLDC Motor in The Modes Without Flux Control and by Using Flux Control

Article · December 2013

CITATION
1

READS
1,034

3 authors, including:



Mohammad Reza Alizadeh Pahlavani
Iran University of Science and Technology, Tehran, Iran
136 PUBLICATIONS 774 CITATIONS

[SEE PROFILE](#)



Peyman Naderi
Shahid Rajaee University
52 PUBLICATIONS 170 CITATIONS

[SEE PROFILE](#)

Some of the authors of this publication are also working on these related projects:



hybrid vehicles [View project](#)



university [View project](#)

The Direct Torque Control of BLDC Motor in the Modes without Flux Control and by Using Flux Control

H. Mirzaei, M. Alizadeh Pahlavani, P. Naderi

Abstract – *The current paper presents the Direct Torque Control (DTC) methods, implemented in six-switch inverter for brushless DC (BLDC) motors with non-sinusoidal back electromotive force, by using two-phase conduction modes. Then, the proposed two-phase conduction mode for DTC of BLDC motors in constant torque area is introduced. In this control method only two phases conduct using a six-phase inverter at any moment of time. Choosing the spatial vectors of inverter voltage in two-phase conduction mode appropriately, the current with a desired waveform is obtained by a simple look-up table. Thus, it is possible to obtain the DTC of a BLDC motor drive with a faster torque response. In this paper, the modeling and simulation of direct torque control and direct flux control with Hall Effect sensor and non-sinusoidal back electromotive force are extensively examined by using a three-phase conduction method and a six-switch inverter.*

Copyright © 2013 Praise Worthy Prize S.r.l. - All rights reserved.

Keywords: Direct Torque Control (DTC), BLDC Motor, Back Electromotive Force (BEMF)

I. Introduction

Permanent magnet synchronous motor (PMSM) drives with sinusoidal back electromotive force and brushless DC (BLDC) motor with trapezoidal back electromotive force, are widely used in many applications. They are widely used in many applications, ranging from Servo drives to transportation drives, because of their several distinct advantages like high power density, high efficiency, high torque to inertia ratio and improved controllability. Brushless DC

(BLDC) Motors Fed by two-phase conduction method, have higher power to weight and torque to current ratios. It is also less costly because of concentrated winding that their coil ends are linked together compared to three-phase feeding permanent magnet synchronous motor (PMSM).

The most well-known way for controlling the BLDC motors, is done by controlling the PWM current, where two-phase feeding method along with a variety of PWM modes, such as soft switching, hard switching and etc is applied. If the waveform of back electromotive force, is an ideal trapezoidal form with 120 degrees electrical conduction and flat top, then three Hall effect sensors are used as position sensor to detect the current commutation points that occur at every 60 electrical degrees. So, according to the cost and high-resolution position sensor (like optical decoder), a relatively low-cost drive compared to PMSM drives is obtained [1]-[3].

For the first time, the Direct torque control technique was proposed by Takahashi and Depenbrock for induction motor drives in the mid 1980s. More than a decade later, in the late 1990s, The DTC technique for Internal synchronous motors (PMSM) were analyzed.

Recently, in order to minimize lower frequency torque ripples and torque response time compared to BLDC motor drives controlled by conventional PWM current, DTC method is widely applied in BLDC motor drives [1], [3].

Voltage space vectors are defined in a two-phase conduction mode and an electromagnetic torque equation in a stationary reference frame is obtained for surface mounted permanent magnet synchronous machines with non-sinusoidal back electromotive force (BLDC and etc).

It is claimed that electromotive torque and the stator flux linkage amplitude of the DTC in BLDC motor under two-phase conduction mode can be controlled simultaneously.

II. The DTC of BLDC

According to Fig. 1, in BLDC motor, back electromotive voltage is a function of rotor position (θ_r) and Amplitude is equal to $E = K_e \cdot \omega_r$ (K_e is the back electromotive voltage constant). Therefore, three-phase back electromotive balanced voltages for any operating point of motor are made by rotor position. During each half-cycle, back electromotive force for 120 electrical degrees, has a constant amplitude while at 60 electrical degrees has a variable amplitude. The flow occurs in each phase when back electromotive voltage of that phase is in its maximum range. Figure 1 shows that only a two-phase flow is established at any point of time and one of the phases is always off. Interestingly, back electromotive voltage in off phase is not fixed and it changes from positive to negative values or vice versa.

BLDC motors are named due to quasi-DC (Square) current existed in per phase of the stator. Given $e_a i_a = T_a \times \omega_m$, creating quasi square current, the torque of each phase is constant in some intervals, which is the same ($K_a \phi i_a$) in DC motors [7]. As a result, the total torque is always constant. The most common method to estimate the rotor position of BLDC motor is using Hall Effect sensors. For BLDC motors with a trapezoidal BEMF, it is enough to obtain location information at every 60° electrical degree interval.

Three Hall effect sensors known as Hall-A, Hall-B, and Hall-C usually are used for a three- phase motor to determine the position of the rotor magnetic field, which each sensor is 120 degrees lag with respect to the previous one. The signals of the sensors are shown in Fig. 1. Generally, the N and S pole signals correspond to '1' and '0', respectively. The basic idea of direct torque control is Selecting the appropriate stator voltage vector of the eight possible inverter modes (proportional to the difference between actual and reference amount of torque and linkage flux), so that the stator flux linkage vector rotates along the stator reference frame (DQ frame) trajectory and produces the desired torque. In two-phase conduction mode, the route of stator flux linkage is ideally predicted hexagonal, as shown in Fig. 2 with a thin line. However, the back electromotive force in a non-stimulated phase transforms straight lines of a hexagonal shape on the stator flux linkage diagram into a curve which tends to the actual trajectory of stator flux linkage and becomes more circular in shape (see Figure 2). Besides rapid changes, curve-like form of flux locus between two consecutive commutations also complicates the stator flux linkage amplitude control, because this feature depends on the size of the fast gradients, and the depth of these changes could be varied due to sampling time, DC link voltage, residual bandwidth, motor parameters particularly the inductance phase, motor speed, snubber circuit and amount of the load torque.

In the constant torque area (under the base rate), it is not rational to change the stator flux linkage amplitude when the back electromotive force of line is lower than DC link voltage. However, at a speed higher than that of base speed, the performance of motor is significantly degraded because the back electromotive force is higher than DC link voltage, and the stator inductance X_s does not allow the phase current to develop quickly enough to catch up to the flat top of the trapezoidal back-EMF.

Desired torque cannot be obtained at speeds over the base speed. If the inductance phase is low, the ripples of torque and current in motor drives controlled by DTC are much higher compared to the machines with a higher inductance phase. Thus, to achieve a lower ripple of current and torque, drive motors controlled by DTC methods with high inductance are preferred [4]. It has also been observed from the stator flux linkage trajectory that when the conventional two-phase PWM flow control is used, fast slopes occur at every 60 electrical degrees due to the inverse parallel performance of diodes.

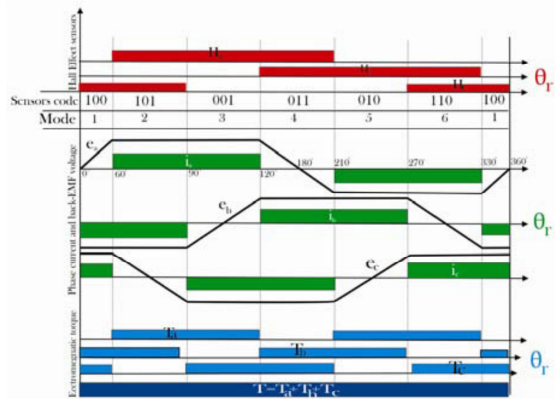


Fig. 1. Synchronization of back electromotive voltage, current stator and torque generated in BLDC motor

The similar phenomena takes into consideration when the DTC method is applied to a BLDC motor, as it is shown in Fig. 2. Due to the fast ramps available in space vector of the stator flux linkage at every commutation (every 60 electrical degrees) and the willingness of currents for adapting to the constant amplitude of the phase back-EMF for smooth torque generation, there is no facile way to control the stator flux linkage amplitude.

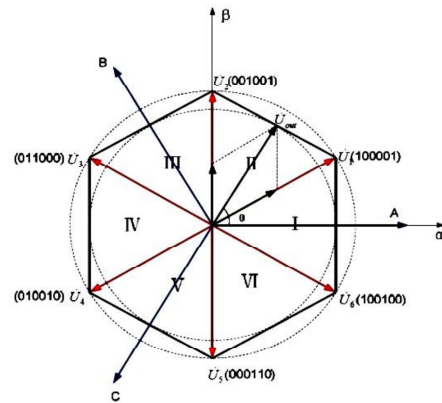


Fig. 2. Routes of the stator flux linkage and two-phase voltage space vectors in stationary reference frame axes $\alpha\beta$ [6]

On the other hand, the rotational speed of the stator flux linkage can be easily controlled in order to obtain fast torque response. The size of such sharp dips is quite unpredictable and depends on various factors.

The best way to control the amplitude of the stator flux linkage is recognizing its actual figure, which doing this in the constant torque area looks very hard.

Therefore, in the DTC of a BLDC motor drive with two-phase conduction scheme, the flux error φ in the voltage vector selection look-up table is always selected as zero and only the torque error τ is used depending on the error level of the actual torque from the reference torque. If the reference torque is bigger than the actual torque, within the hysteresis bandwidth, the torque error τ is defined as "1," otherwise it is "-1", as shown in Table I.

TABLE I
TWO-PHASE VOLTAGE VECTOR SELECTION FOR BLDC MOTOR

		0					
φ	τ	θ_1	θ_2	θ_3	θ_4	θ_5	θ_6
1	1	$V_1(100001)$	$V_2(001001)$	$V_3(011000)$	$V_4(010010)$	$V_5(000110)$	$V_6(100100)$
	-1	$V_6(100100)$	$V_1(100001)$	$V_2(001001)$	$V_3(011000)$	$V_4(010010)$	$V_5(000110)$
0	1	$V_2(001001)$	$V_3(011000)$	$V_4(010010)$	$V_5(000110)$	$V_6(100100)$	$V_1(100001)$
	-1	$V_5(000110)$	$V_6(100100)$	$V_1(100001)$	$V_2(001001)$	$V_3(011000)$	$V_4(010010)$
-1	1	$V_3(011000)$	$V_4(010010)$	$V_5(000110)$	$V_6(100100)$	$V_1(100001)$	$V_2(001001)$
	-1	$V_4(010010)$	$V_5(000110)$	$V_6(100100)$	$V_1(100001)$	$V_2(001001)$	$V_3(011000)$

III. The Control with Flux and without Flux in DTC of BLDC Motor

The block diagram of the closed-loop DTC in BLDC motor drive in the constant torque region is shown in Figure 3. The highlights represent the stator flux linkage control part which is used only to perform comparison. When the key in Figure 3 is shifted from mode 2 into mode 1, the flux control and torque control are simultaneously taken into consideration.

Each block is described according to the Figure 3.

III.1. Modeling the Residual Torque and Flux Controllers

Fig. 3 depicts the overall block diagram schematic of the DTC for BLDC motors. The stator command flux and torque magnitudes (T_{em}^* , λ_s^*) are compared with their respective estimated values. The errors are then processed through two hysteresis controllers which operate independently of each other (one for flux and one for torque). The flux and torque controllers are two- and three-level controllers, respectively. The hysteresis torque control in six time intervals for both torque error

polarities (positive and negative) are shown in Figs. 4 and 5.

According to Figs. 4 and 5, in order to obtain the fast dynamic control of motor torque, the residual torque and flux controllers method is applied, where ‘2h’ is the overall bandwidth of the residual torque controller, and ‘e’ is the differential magnitude between the actual and base values. The torque controller block has been modeled by embedded functions in Matlab/Simulink environment according to Fig. 6.

III.2. Mode of Switching and Selecting the Voltage Vector

6 non-zero voltage space vectors which are used in six-switch DTC of BLDC motor drive can be shown as follows:

$$V_x = (S_1, S_2, S_3, S_4, S_5, S_6) \quad (1)$$

in which x is between 1 and 6, and S_1, \dots, S_6 are key modes. ‘1’ shows ON mode, and ‘0’ shows the OFF mode in respective key.

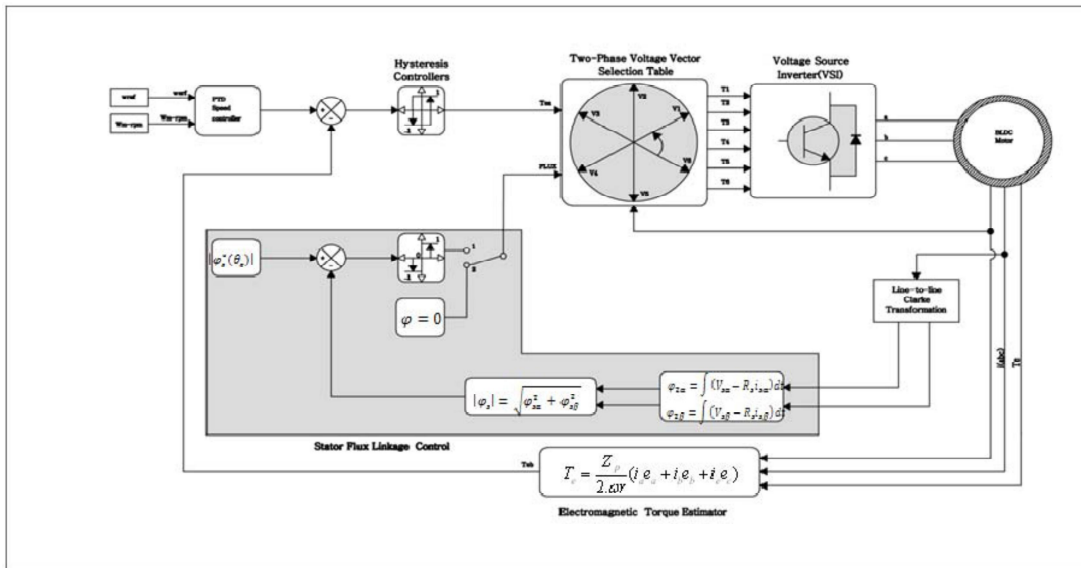


Fig. 3. The block diagram of the closed-loop DTC in BLDC motor drive in the constant torque region

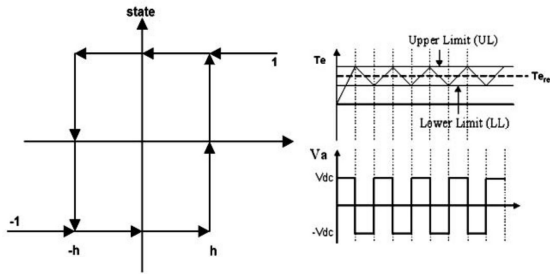


Fig. 4. Dihedral torque hysteresis controller

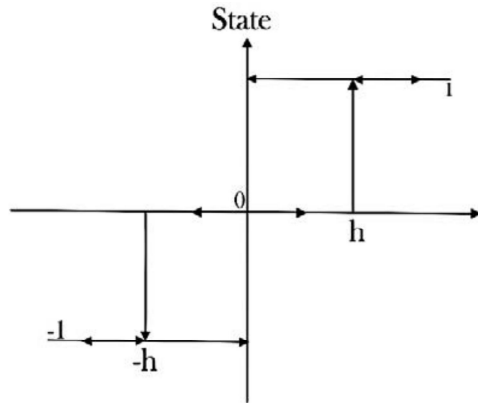


Fig. 5. The three-level flux hysteresis controller

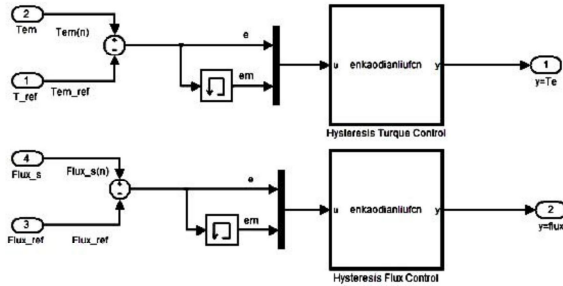


Fig. 6. Blocks of hysteresis torque and flux controllers

According to Eq. (2) and Figs. 5 and 6, the switching functions of 6 non-zero voltage space vectors V_1, V_2, \dots, V_6 in 6-switch DTC of BLDC motor drive in abc frame, can be obtained as follows:

$$V_1(100001) \Rightarrow V_{1a} = V_{dc}, V_{1b} = 0, V_{1c} = -V_{dc} \quad (2)$$

$$V_2(001001) \Rightarrow V_{2a} = 0, V_{2b} = V_{dc}, V_{2c} = -V_{dc} \quad (3)$$

$$V_3(011000) \Rightarrow V_{3a} = -V_{dc}, V_{3b} = V_{dc}, V_{3c} = 0 \quad (4)$$

$$V_4(010010) \Rightarrow V_{4a} = -V_{dc}, V_{4b} = 0, V_{4c} = V_{dc} \quad (5)$$

$$V_5(000110) \Rightarrow V_{5a} = 0, V_{5b} = -V_{dc}, V_{5c} = V_{dc} \quad (6)$$

$$V_6(100100) \Rightarrow V_{6a} = V_{dc}, V_{6b} = -V_{dc}, V_{6c} = 0 \quad (7)$$

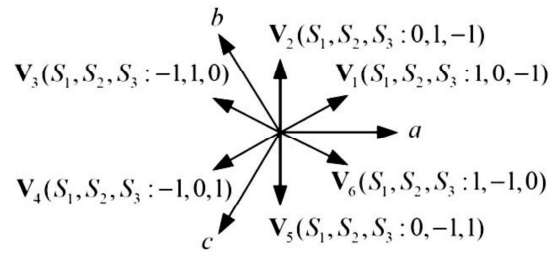


Fig. 7. DTC voltage vectors [5]

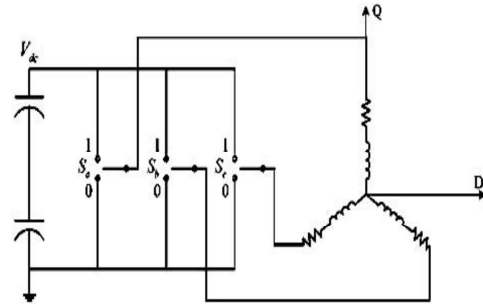


Fig. 8. Electric circuit of six-switch drive

$$\begin{aligned} v_a &= \frac{1}{3} V_{dc} (2S_a - S_b - S_c) \\ v_b &= \frac{1}{3} V_{dc} (-S_a + 2S_b - S_c) \\ v_c &= \frac{1}{3} V_{dc} (-S_a - S_b + 2S_c) \end{aligned} \quad (8)$$

In stationary reference frame, $(V_{x\alpha}, V_{x\beta})$ can be achieved as follows. And also Eq. (9) can be applied to prove Clark's transform vector equations:

$$\begin{pmatrix} X_\alpha \\ X_\beta \end{pmatrix} = \frac{2}{3} \begin{bmatrix} 1 & -\frac{1}{2} & -\frac{1}{2} \\ 0 & \sqrt{3} & -\frac{\sqrt{3}}{2} \end{bmatrix} \begin{pmatrix} X_a \\ X_b \\ X_c \end{pmatrix} \quad (9)$$

$$V_1(100001) \Rightarrow V_{1\alpha} = V_{dc}, V_{1\beta} = \frac{V_{dc}}{\sqrt{3}} \quad (10)$$

$$V_2(001001) \Rightarrow V_{2\alpha} = 0, V_{2\beta} = \frac{2}{\sqrt{3}} V_{dc} \quad (11)$$

$$V_3(011000) \Rightarrow V_{3\alpha} = -V_{dc}, V_{3\beta} = \frac{-V_{dc}}{\sqrt{3}} \quad (12)$$

$$V_4(010010) \Rightarrow V_{4\alpha} = -V_{dc}, V_{4\beta} = -\frac{V_{dc}}{\sqrt{3}} \quad (13)$$

$$V_5(000110) \Rightarrow V_{5\alpha} = 0, V_{5\beta} = -\frac{2}{\sqrt{3}} V_{dc} \quad (14)$$

$$V_6(100100) \Rightarrow V_{6\alpha} = V_{dc}, V_{6\beta} = \frac{V_{dc}}{\sqrt{3}} \quad (15)$$

As shown in Table I, if the reference torque is greater than the actual torque, within the hysteresis bandwidth, the torque error τ is defined as “1,” otherwise it is “-1” and considering Table I and Fig. 8, the switching mode in 6-switch inverter can be modeled and simulated, same as Fig. 9.

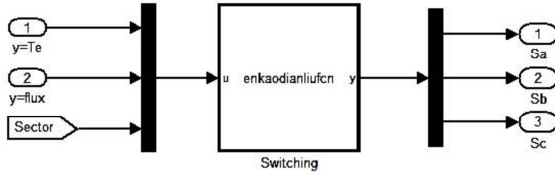


Fig. 9. Simulated block diagram of switching scheme in six-switch inverter

III.3. How to Create Voltage Source Inverter

As shown in Fig. 10, in three-phase BLDC motor, inverter is described by the following set of equations, and in order to obtain the voltage source inverter, Fig. 6 and the following equations are used.

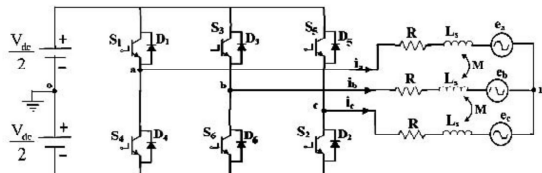


Fig. 10. Structure of BLDC Motor six-switch inverter

$$\begin{bmatrix} v_{an} \\ v_{bn} \\ v_{cn} \end{bmatrix} = \begin{bmatrix} R & 0 & 0 \\ 0 & R & 0 \\ 0 & 0 & R \end{bmatrix} \begin{bmatrix} i_{sa} \\ i_{sb} \\ i_{dc} \end{bmatrix} + \\ + \begin{bmatrix} L - M & 0 & 0 \\ 0 & L - M & 0 \\ 0 & 0 & L - M \end{bmatrix} \frac{d}{dt} \begin{bmatrix} i_{sa} \\ i_{sb} \\ i_{dc} \end{bmatrix} + \begin{bmatrix} e_a \\ e_b \\ e_c \end{bmatrix} \quad (16)$$

According to Fig. 10, terminals voltage relative to the ground point (0) can be represented by following equation in matrix form:

$$\begin{bmatrix} v_{ao} \\ v_{bo} \\ v_{co} \end{bmatrix} = \begin{bmatrix} R & 0 & 0 \\ 0 & R & 0 \\ 0 & 0 & R \end{bmatrix} \begin{bmatrix} i_{sa} \\ i_{sb} \\ i_{dc} \end{bmatrix} + \\ + \begin{bmatrix} L - M & 0 & 0 \\ 0 & L - M & 0 \\ 0 & 0 & L - M \end{bmatrix} \frac{d}{dt} \begin{bmatrix} i_{sa} \\ i_{sb} \\ i_{dc} \end{bmatrix} + \begin{bmatrix} e_a \\ e_b \\ e_c \end{bmatrix} + \begin{bmatrix} v_{no} \\ v_{no} \\ v_{no} \end{bmatrix} \quad (17)$$

If Eq. (16) is inserted in (17), and star point voltage relative to the ground is zero, then:

$$v_{no} = \frac{v_{ao} + v_{bo} + v_{co} - (e_a + e_b + e_c)}{3} \quad (18)$$

According to the above equations, the voltage source inverter can be modeled.

IV. Simulation Results

IV.1. Direct Torque Control, without Flow Control

First, we consider the case in which torque control has been implemented and flux control ignored.

Figs. 11, 12, 13 and 14 show the diagram of the stator flux linkage for ($\alpha\beta$) axis in the case which rate of speed is respectively 30, 100, 150 and 300 electric [rpm] and the load torque at every figure is equal to 0, 5, 9 and 12 [Nm]. According to the figures, it can be observed that, by increasing the torque at a constant speed, the torque ripple increases.

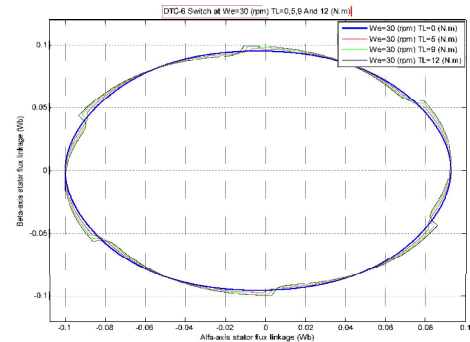


Fig. 11. Diagram of the stator flux linkage for ($\alpha\beta$) axis with speed rate of 30[rpm]

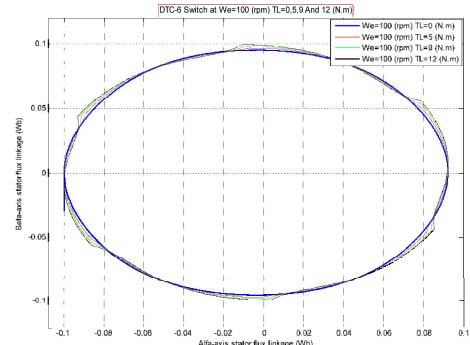


Fig. 12. Diagram of the stator flux linkage for ($\alpha\beta$) axis with speed rate of 100[rpm]

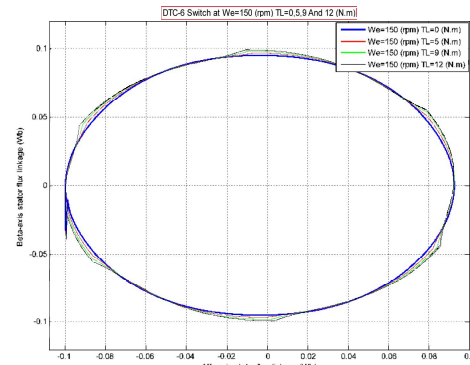


Fig. 13. Diagram of the stator flux linkage for ($\alpha\beta$) axis with speed rate of 150[rpm]

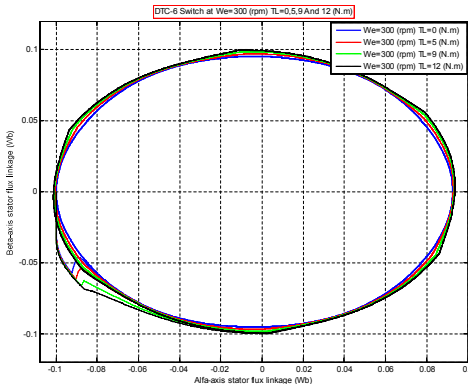


Fig. 14. Diagram of the stator flux linkage for ($\alpha\beta$) axis with speed rate of 300[rpm]

According to Fig. 14, if we increase the speed at a rated speed, the torque ripple at the torque of different loads becomes lower; therefore, BLDC motor at low speed has higher torque ripple than the mode with higher speed. Figs. 15, 16, 17 and 18 show the diagram of the stator flux linkage for ($\alpha\beta$) axis in the case which the load torque is equal to 0, 5, 9 and 12 [Nm], and the speed at every figure is equal to 30, 10, 150 and 300 electric [rpm] respectively.

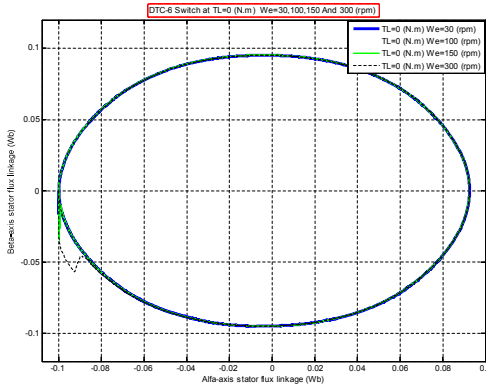


Fig. 15. Diagram of the stator flux linkage for ($\alpha\beta$) axis with load torque equal to 0[Nm]

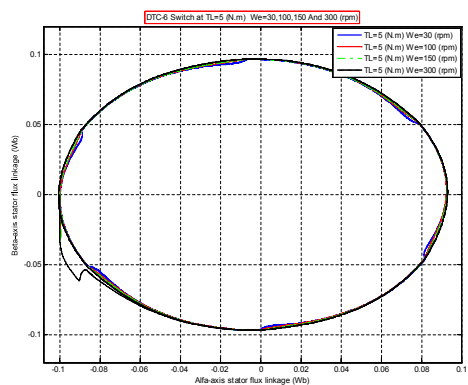


Fig. 16. Diagram of the stator flux linkage for ($\alpha\beta$) axis with load torque equal to 5[Nm]

As it can be seen from the figures, by increasing speed at constant load torque, torque ripple at speeds close to the rated speed is much lower than torque ripple at low speeds due to the poor performance of the BLDC motor at low speeds. We also see in the figures that in the mode without flow control, the flux amplitude remains constant by changing the speed and the load torque.

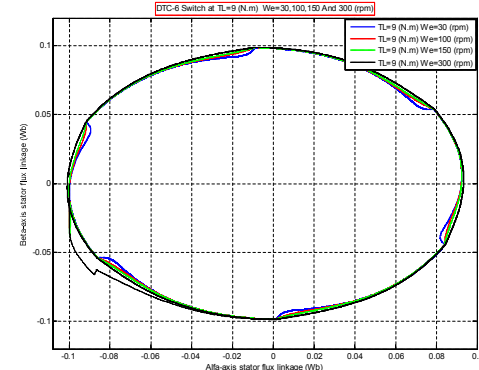


Fig. 17. Diagram of the stator flux linkage for ($\alpha\beta$) axis with load torque equal to 9[Nm]

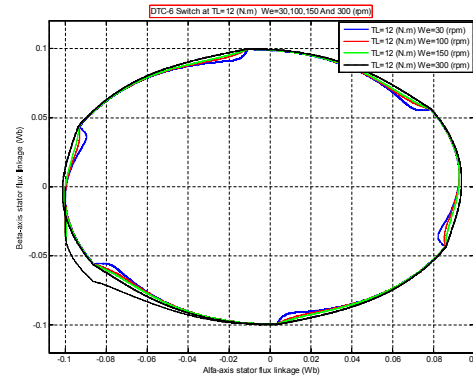


Fig. 18. Diagram of the stator flux linkage for ($\alpha\beta$) axis with load torque equal to 12[Nm]

IV.2. Direct Torque Control, with Flux Control

In this section we consider the case in which both torque control and flux control is implemented.

Figs. 19, 20, 21 and 22 show the diagram of the stator flux linkage for ($\alpha\beta$) axis in the case which the speed is equal to 30, 100, 150 and 300 electric [rpm] and the load torque at every figure is respectively equal to 0, 5, 9 and 12 [Nm].

According to the figures, it can be concluded that by increasing the load torque, flux amplitude increases, and based on the Fig. 19, lower the speed, flux more weakened and it shows itself as a hexagonal form. Also according to Fig. 21, when the speed is 150 [rpm] and the load torque is 5 [Nm], a more circular shape is obtained and if we increase the torque in this mode, the torque ripple increases higher.

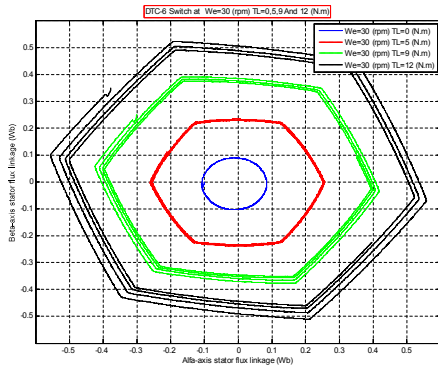


Fig. 19. Diagram of the stator flux linkage for ($\alpha\beta$) axis which the speed is equal to 30[rpm]

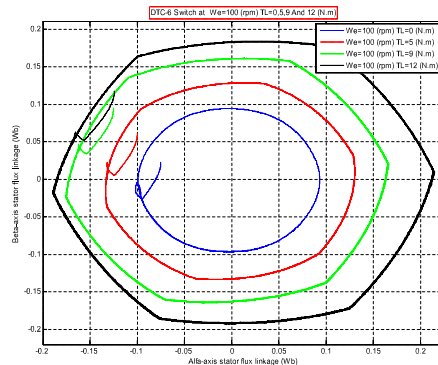


Fig. 20. Diagram of the stator flux linkage for ($\alpha\beta$) axis which the speed is equal to 100[rpm]

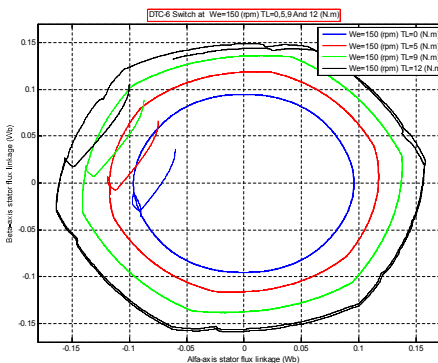


Fig. 21. Diagram of the stator flux linkage for ($\alpha\beta$) axis which the speed is equal to 150[rpm]

According to Fig. 22, at the electric speed of 300 [rpm], when load torque is increased from zero to higher degrees, the diagram of stator flux linkage for ($\alpha\beta$) axis is out of its circle mode route and the system loses its ability to control torque.

Figs. 23, 24, 25 and 26 show the diagram of the stator flux linkage for ($\alpha\beta$) axis in the mode which the load torque is respectively equal to 0, 5, 9 and 12 [Nm] and the speed at every figure is equal to 30, 100, 150 and 300 electric [rpm].

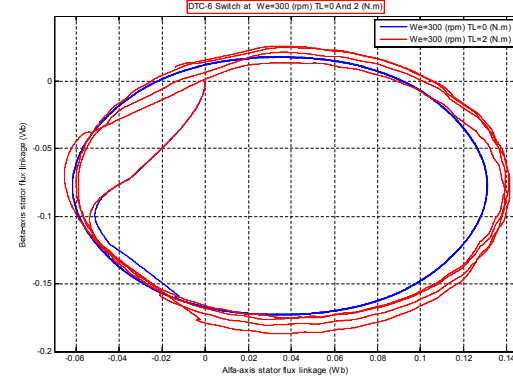


Fig. 22. Diagram of the stator flux linkage for ($\alpha\beta$) axis which the speed is equal to 300[rpm]

As it could be seen from the figure, by increasing speed, the torque is constant and flux amplitude is reduced, and according to Fig. 24, when the speed and the torque are respectively 300 [rpm] and 5 [Nm], flux control gives the best results.

The poor performance of BLDC motors at low speed can be seen in these figures, as well.

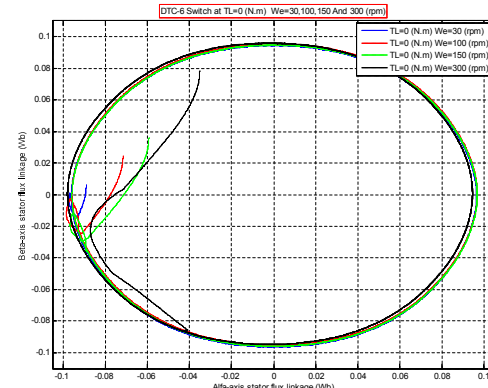


Fig. 23. Diagram of the stator flux linkage for ($\alpha\beta$) axis which the load torque is respectively equal to 0[Nm]

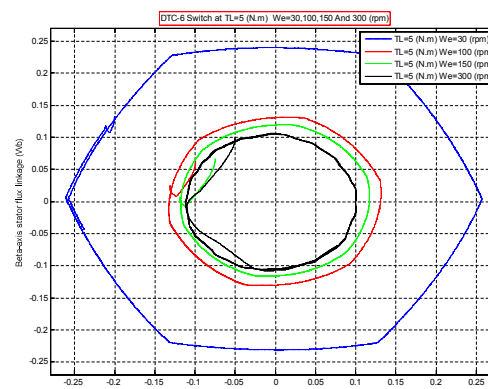


Fig. 24. Diagram of the stator flux linkage for ($\alpha\beta$) axis which the load torque is respectively equal to 5[Nm]

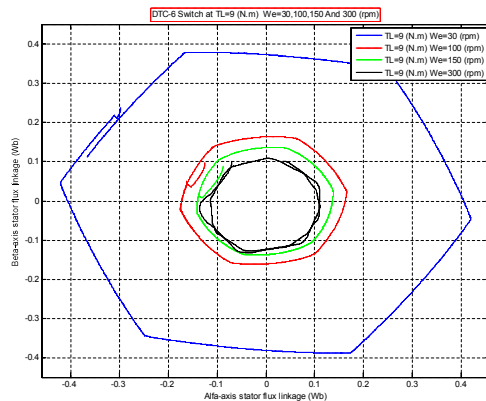


Fig. 25. Diagram of the stator flux linkage for ($\alpha\beta$) axis which the load torque is respectively equal to 9[Nm]

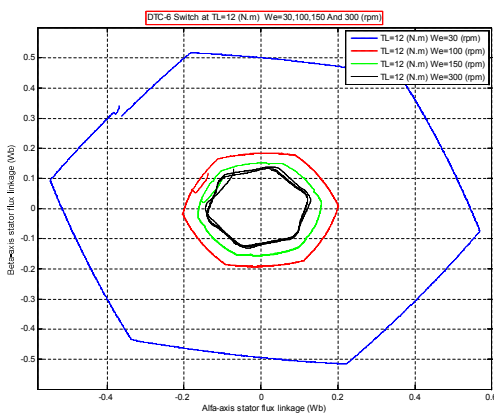


Fig. 26. Diagram of the stator flux linkage for ($\alpha\beta$) axis which the load torque is respectively equal to 12[Nm]

V. Conclusion

The present study successfully has attempted to describe the application of the proposed two-phase conduction direct torque control (DTC) method for BLDC motor drivers in constant torque region. A look-up table is designed for choosing a two-phase voltage vector, in order to provide a faster torque response in terms of both bullish and bearish conditions. This method, compared to three-phase DTC, eliminates the flux control and only torque is considered in the overall control system.

Three reasons are given for removing the flux control. First, since the line-to-line back-EMF including small voltages drop is lower than the dc-link voltage in the constant torque region, there is no need to control flux amplitude. Second, with the two-phase conduction mode, sudden sharp dips in the stator flux linkage locus occur that due to their unpredictability complicate the control scheme.

Third, regardless of the stator flux linkage amplitude, the phase currents tend to adapt to the flat top portion of the corresponding trapezoidal back-EMF to generate a constant torque.

References

- [1] Salih Baris Ozturk,, "Direct Torque Control Of Permanent Magnet Synchronous Motors With Non-Sinusoidal Back-EMF," Submitted to the Office of Graduate Studies of Texas A&M University in partial fulfillment of the requirements for the degree of DOCTOR OF PHILOSOPHY, May 2008.
- [2] Salih Baris Ozturk, Member, IEEE, and Hamid A. Toliyat, Fellow, IEEE, "Direct Torque and Indirect Flux Control of Brushless DC Motor, " IEEE/ASME TRANSACTIONS ON MECHATRONICS, VOL. 16, NO. 2, APRIL 2011.
- [3] S. B. Ozturk and H. A. Toliyat, "Direct torque control of brushless dc motor with non-sinusoidal back EMF," in Proc. IEEE IEMDC Biennial Meet., Antalya, Turkey, May 3–5, 2007, vol. 1, pp. 165–171.
- [4] Y. Liu, Z. Q. Zhu, and D. Howe, "Direct torque control of brushless dc drives with reduced torque ripple," IEEE Trans. Ind. Appl., vol. 41, no. 2, pp. 599–608, Mar./Apr. 2005.
- [5] Diansheng Sun, "Research on Torque Direct Control Method for Brushless DC Motors with Non-ideal Back EMF Waveforms," 978-1-4577-0536-6/11/\$26.00 ©2011 IEEE.
- [6] Qiang Wu, Guangwei Meng , Hao Xiong, Huaihua Li and Libing Zhou, "A Novel Starting Control for Sensorless Three-Phase Permanent-Magnet Brushless DC Motor," 978-1-4244-8039-5/11/\$26.00 ©2011 IEEE.
- [7] A. Halvaei Niasar; "Control Brushless DC Motor ",Nishabor University of Iran 2011.

Hassan Mirzaei received his M.S. degree in electrical engineering from Boroujerd Science and Research, Islamic Azad University, in 2013. He is Researcher in field of electrical machines. Boroujerd Science and Research, Islamic Azad university, Boroujerd, Iran.
E-mail: Hassan.mirzaei.ep@gmail.com

Mohammad Reza Alizadeh Pahlavani received his Ph.D. degree in electrical engineering from Iran University of Science and Technology (IUST) in 2009. He is the author of more than 110 journal and conference papers in field of electromagnetic systems, electrical machines, power electronic, FACTS devices, and pulsed power. Malek-Ashtar University of Technology (MUT), Shabanlo St., Lavizan, Tehran, Iran.
E-mail: Mr_Alizadchp@iust.ac.ir

Peyman Naderi was born in Ahvaz,Iran, in 1975. He received his B.S.degree in Electronic Engineering in1998 and M.S. degree in Power Engineering from Chamran University, Iran, Ahvaz in 2001. He has a Ph.D. degree in Power Engineering Science from K.N. Toosi University, Tehran, Iran. His interests are hybrid and electric vehicles, vehicles dynamic, power system transients and power system dynamics. He is currently assistant professor in Shahid Rajaee Teacher Training University of Tehran, Iran.
E-mail: p.naderi@srttu.edu